

Supporting Information

Modulating Room-Temperature Phosphorescence of Triazine-Carbazole Systems with Stimuli-Responsive Behaviors through Conjugation Expanding

Qu Fu^[a], Longjian Wu^[a], Yuxi Wang^[a], Lingbo Kong^[a], Zhenli Guo^[b], Chao Zheng^{[b]}, Runfeng Chen^{*[a, b]}*

^[a]School of Materials Science and Engineering, Zhejiang Sci-Tech University, Hangzhou 310018, China

^[b]State Key Laboratory of Organic Electronics and Information Displays & Institute of Advanced Materials (IAM), Nanjing University of Post & Telecommunications, 9 Wenyuan Road, Nanjing 210023, China

Corresponding Author

Runfeng Chen E-mail: iamczheng@njupt.edu.cn; iamrfchen@njupt.edu.cn

Contents

1. Materials and structural characterizations	S2
2. Synthesis and Characterization	S2
3. Photophysical property measurements	S5
4. Sample Preparation.....	S5
5. Computational details.....	S5
6. Applications.....	S6
7. Figures	S6
8. Tables	S12
9. References	S13

1. Materials and structural characterizations

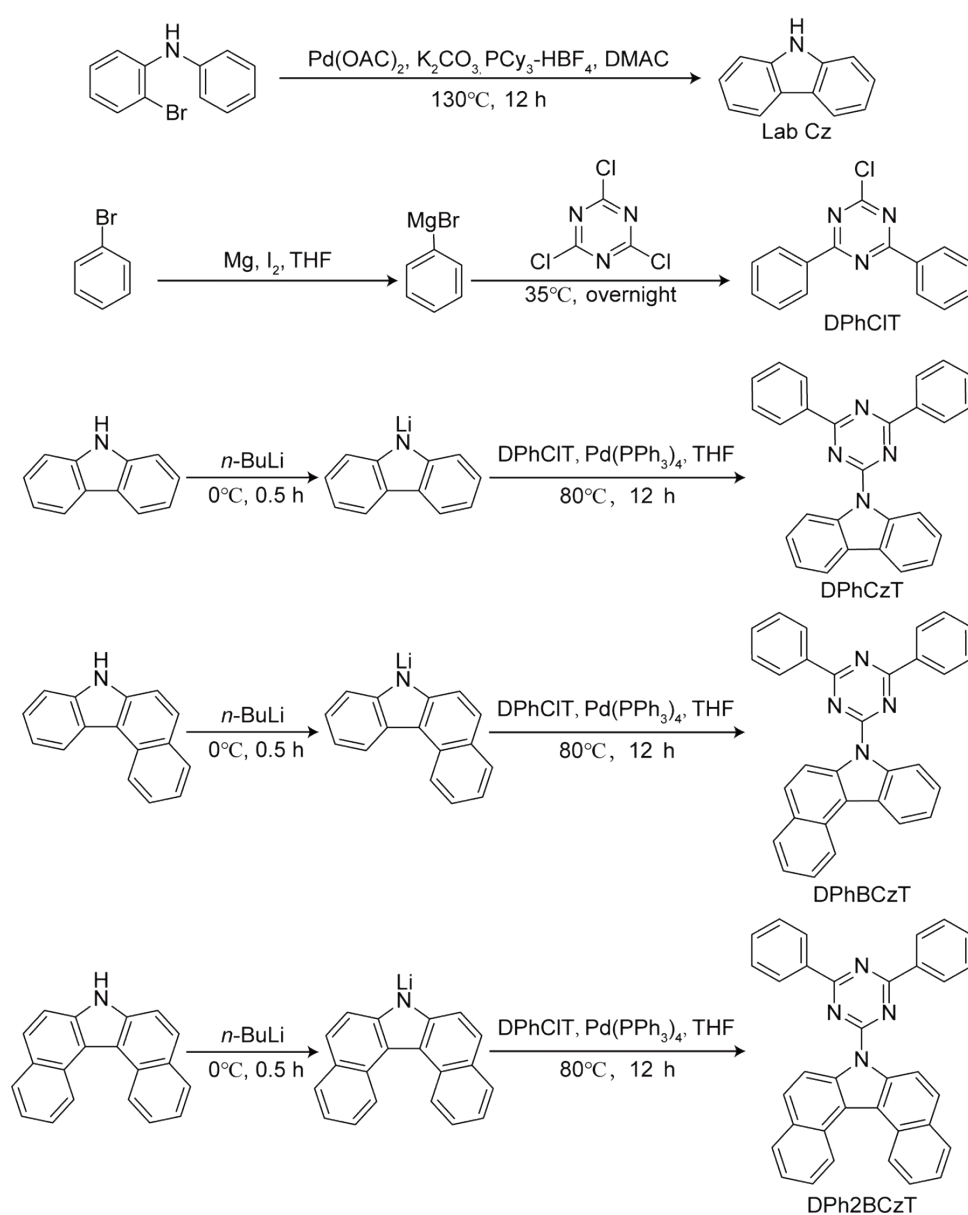
Unless otherwise mentioned, materials were used without further purification. 2-Bromodiphenylamine, potassium carbonate (K_2CO_3), palladium(II) acetate ($Pd(OAc)_2$), tricyclohexylphosphine tetrafluoroborate (PCy_3-HBF_4), 1.6 M hexane solution of *n*-butyllithium, carbazole, 7H-benzo[*c*]carbazole, ultra-dry tetrahydrofuran (THF), iodine, 2-bromo-*N*-phenylbenzenamine, dimethylacetamide (DMAC), hexane (Hex), toluene (Tol), dibutyl ether (DBE), chlorobenzene (CB), 1,2-dichlorobenzene (*O*-DCB), dichloromethane (DCM), ethanol (EtOH), acetonitrile (ACN) were purchased from MACKLIN, while 2-chloro-4,6-diphenyl-1,3,5-triazine, bromobenzene, cyanuric chloride, and magnesium turnings were purchased from Aladdin. Tetrakis(triphenylphosphine)palladium ($Pd(PPh_3)_4$), 7H-dibenzo[*c,g*]carbazole were from Leyan. Milli-Q-Millipore water was employed in all the experiments. Silica gel (0.0385–0.05 mm) was used in column chromatography. The prepared new molecules were characterized by nuclear magnetic resonance (1H NMR and ^{13}C NMR) spectra (Bruker AVANCE AV400MHz spectrometer), and high resolution mass spectrometry (HRMS) (Thermo Scientific Q Exactive). Single-crystal X-ray diffraction (XRD) data were collected using the Xeuss 2.0 (Xenocs, France) with an incident X-ray Cu- $K\alpha$ beam ($\lambda = 1.54189 \text{ \AA}$). Thermogravimetric (TGA) analyses were performed on a TGA 550 with a heating rate of $10^\circ C \cdot min^{-1}$ in a nitrogen atmosphere.

2. Synthesis and Characterization

The isomer-free laboratory carbazole (Lab Cz), 6-chloro-2,4-di(*N,N*-diphenyl)-1,3,5-triazine (DPhCIT), 4,6-diphenyl-2-carbazolyl-1,3,5-triazine (DPhCzT), 4,6-diphenyl-2-benzo[*c*]carbazolyl-1,3,5-triazine (DPhBCzT) and 4,6-diphenyl-2-dibenzo[*c,g*]carbazolyl-1,3,5-triazine (DPh2BCzT) were synthesized according to the following synthetic route (Scheme S1).

Laboratory carbazole (Lab Cz): According to a reported synthetic route^{1,2}, K_2CO_3 (1.10 g, 8 mmol), $Pd(OAc)_2$ (26.9 mg, 0.12 mmol), and PCy_3-HBF_4 (88.4 mg, 0.24 mmol) were added to a 100 mL bottle, which was degassed and filled with nitrogen for 3 times. Then, 2-bromo-*N*-phenylbenzenamine (1.00 g, 4 mmol) which was dissolved in DMAC (10 mL) was added to the bottle. The mixed solution was refluxed at $130^\circ C$ for 16 h in a nitrogen atmosphere. After the reaction was completed, the resultant mixture was cooled down to room temperature and extracted with DCM for 3 times. The combined organic phase was dried over Na_2SO_4 and the solvents were removed by rotary evaporation. The crude product was purified by column chromatography using petroleum ether:ethyl acetate (50:1, v/v) to obtain pure product as white powder (0.40 g, 60% yield).

6-Chloro-2,4-di(N,N-diphenyl)-1,3,5-triazine (DPhCIT): Following the synthetic method reported previously^{3,4}, bromobenzene (5.80 mL, 55.4 mmol) was added slowly to a stirred mixture of magnesium turnings (1.38 g, 57.5 mmol) in dry THF (20 mL) containing a catalytic amount of iodine under nitrogen to obtain the Grignard reagent. The Grignard reagent solution was dropped slowly into a stirred solution of cyanuric chloride (3.00 g, 16.2 mmol) in dry THF (20 mL) at 35°C. After stirring for 12 h, the mixture was poured into water and extracted with DCM for 3 times. The organic layers were collected, combined and dried over Na₂SO₄. The solvent was removed by rotary evaporation, and the residue was purified by flash column chromatography to give DPhCIT (2.18 g, 50% yield) as a white solid.



Scheme S1. Synthesis of Lab Cz, DPhCIT, DPhCzT, DPhBCzT and DPh2BCzT.

4,6-Diphenyl-2-carbazolyl-1,3,5-triazine (DPhCzT): In a 50 mL round-bottomed flask equipped with a magnetic agitator, commercial carbazole (150 mg, 0.90 mmol) was dissolved in 5 mL ultra-dry THF by continuous stirring for 10 min under the protection of nitrogen atmosphere. The solution was cooled to 0°C by an icy bath, after which a 1.6 M hexane solution of *n*-butyllithium (0.56 mL, 0.90 mmol) was added slowly. The resulting mixture was stirred and reacted at 0°C for 10 min, after which the mixture was allowed to warm to room temperature to yield a yellow slurry of lithium carbazolidate. Then, a mixture of DPhCIT (0.20 g, 0.75 mmol) and Pd(PPh₃)₄ (93 mg, 0.08 mmol) dissolved in THF (5 mL) was added slowly to the flask, resulting in the precipitation of solid products. After 30 min, the mixture was heated up to 80°C and reacted at this temperature overnight to improve the yield. The precipitation was collected and washed with water and acetone for several times. Recrystallization of the solid in chlorobenzene to afford DPhCzT (0.20 g, 65% yield) as a white powder.

4,6-Diphenyl-2-Benzo[*c*]carbazolyl-1,3,5-triazine (DPhBCzT): Following the identical synthetic procedure of DPhCzT, **DPhBCzT** was obtained by the reaction of 7H-benzo[*c*]carbazole (200 mg, 0.90 mmol), 1.6 M hexane solution of *n*-butyllithium (0.56 mL, 0.90 mmol), DPhCIT (0.20 g, 0.75 mmol) and Pd(PPh₃)₄ (93 mg, 0.08 mmol) at 80°C overnight. The reaction mixture was quenched by water (50 mL) and extracted using DCM for 3 times. The organic phase was collected, combined and dried using anhydrous Na₂SO₄. The organic solvents were removed by rotary evaporation and the crude product was purified by column chromatography using petroleum ether:ethyl acetate (10:1, v/v) to afford DPhBCzT in a white solid (260 mg, 87% yield). ¹H NMR (400 MHz, CDCl₃) δ 9.28 (d, *J* = 9.2 Hz, 1H), 9.21 - 9.18 (m, 1H), 8.90 (dd, *J* = 8.5 and 1.0 Hz, 1H), 8.82 - 8.76 (m, 4H), 8.68 - 8.63 (m, 1H), 8.08 - 8.01 (m, 2H), 7.75 (ddd, *J* = 8.4, 6.9, and 1.4 Hz, 1H), 7.70 - 7.54 (m, 9H). ¹³C NMR (101 MHz, CDCl₃) δ 172.50, 165.13, 138.65, 137.25, 136.03, 132.81, 130.77, 129.14, 129.01, 128.97, 128.81, 127.69, 127.05, 126.95, 125.64, 124.40, 123.68, 123.51, 121.96, 119.51, 117.09. HRMS: *m/z* [M+H⁺] calculated for C₃₁H₂₀N₄, 448.1688; found, 448.1697.

4,6-Diphenyl-2-Dibenzo[*c,g*]carbazolyl-1,3,5-triazine (DPh2BCzT): Following the identical preparation procedure of DPhBCzT, **DPh2BCzT** was achieved using 7H-Dibenzo[*c,g*] carbazole (240 mg, 0.9 mmol), 1.6 M hexane solution of *n*-butyllithium (0.56 mL; 0.90 mmol), DPhCIT (0.20 g; 0.75 mmol) and Pd(PPh₃)₄ (93 mg; 0.08 mmol). The prepared DPh2BCzT was a yellow solid (186 mg, 50% yield). ¹H NMR (400 MHz, CDCl₃) δ 9.18 (d, *J* = 9.1 Hz, 2H), 9.12 (d, *J* = 8.5 Hz, 2H), 8.85 - 8.79 (m, 4H), 8.07 (dd, *J* = 14.2 and 8.5 Hz, 4H), 7.73 - 7.56 (m, 10H). ¹³C NMR (101 MHz, CDCl₃) δ 172.73, 165.04, 136.82, 135.80, 132.99, 131.23, 129.17, 128.86, 128.69, 128.18, 127.30, 126.00, 125.23, 124.50, 121.28, 116.16. HR-MS: *m/z* [M+H⁺] calculated for C₃₅H₂₂N₄, 498.1844; found, 498.1853.

3. Photophysical property measurements

The ultraviolet-visible (UV-Vis) absorption spectra was measured on a U-3600PLUS, 230 V Spectrophotometer (Shimadzu). Photographs were taken by a Sony a6000. Steady-state photoluminescent (SSPL) spectra, phosphorescent spectra, kinetic scanings and luminescent lifetimes, time-resolved emission scanning spectrum and excitation-phosphorescence mapping were obtained on an Edinburgh FLS 1000 spectrophotometer equipped with a xenon arc lamp (Xe900) and a microsecond flash-lamp(μ F900) and a picosecond pulsed light emitting diodes with several wavelengths. Absolute total photoluminescence quantum yields (PLQYs) were measured on the FLS 1000 device using an integrating sphere including both fluorescence and phosphorescence emission components. The excitation-phosphorescence spectra were collected on a HITACHI F-4700 fluorescence spectrophotometer under ambient conditions.

4. Sample Preparation

DPh2BCzT@PMMA films with different doping contents were prepared in the following procedure. Two solutions of PMMA (500 mg) and DPh2BCzT (5 mg) were prepared by dissolved them in 5 mL DCM. The two solutions were mixed at different volume ratios and the resulting mixture was ultrasounded for 5 min at room temperature. The mixed solution was cast into a mold and after 30 min, the mold was heated at 80°C in an oven for 180 min to ensure the complete solvent evaporation to form transparent films of DPh2BCzT@PMMA with different contents of DPh2BCzT. DPhBCzT@PMMA and DPhCzT@PMMA films were prepared by the same procedure.

5. Computational details

Density functional theory (DFT) and time-dependent DFT (TD-DFT) calculations were performed to investigate the frontier molecular orbital energy levels and their distributions using Gaussian 09 package.^[2] The functional of Lee Yang Parr's correlation functional (B3LYP) was adopted to optimize the ground state (S_0) geometry with the 6-31G(d) basis set. The optimized structure was further characterized by harmonic vibrational frequency analysis to confirm that real local minimum without any imaginary frequency was reached at the same computational level. The energies of the lowest singlet excited state (S_1) and triplet excited state (T_n) as well as the frontier molecular orbital distributions of the highest occupied molecular orbital (HOMO) and the lowest unoccupied molecular orbital (LUMO) were computed by B3LYP/6-31G(d) based on optimized S_0 structure. The spin-orbit coupling (SOC) values were computed using ORCA version 5.0 software with the M062x generalized functional and cc-pVDZ basis set based on the optimized S_0 geometry. Natural transition orbital (NTO) analyses were conducted on the basis of S_0 geometry using pbe1pbe functional and 6-31g(d,p) basis set.

6. Applications

The preparation and application of smart paper

The smart paper was prepared by coating a mixed DCM solution of PMMA and DPh2BCzT with a doping content of 0.5 wt% on a substrate of glass. UV masks whose the middle part is a transparent pattern while the surrounding area is opaque were design and prepared with patterns of heart, five-pointed star, and dragonfly, respectively. The mask was then placed on the smart paper and activated using a 365 nm UV lamp for 10 s to print a series of different patterns. After removal of the UV masks, the printed patterns on the smart paper cannot be observed under daylight but can be clearly observed when the smart paper is UV irradiated and turned off to show the afterglow. The patterns on the smart paper can be erased in air after several minutes, and other patterns can be printed on the smart paper again using the differently patterned UV masks to achieve different afterglow patterns. Notably, the printed patterns will be maintained in the smart paper for several minutes at room temperature, serving as a Snapchat application.⁵

Morse code information encryption⁶

First, square films of DPhCzT@PMMA-0.5%, DPhBCzT@PMMA-1% and DPh2BCzT@PMMA-0.5% were prepared. Then, they were arranged in a 4×4 matrix in a certain order. After different photoactivation time using a 365 nm UV lamp, the matrix displays different information in the steady state and delayed emission modes to realize time-resolved information encryption, when assigning specific colors to the Morse code symbols of “•” and “-”, respectively.

7. Figures

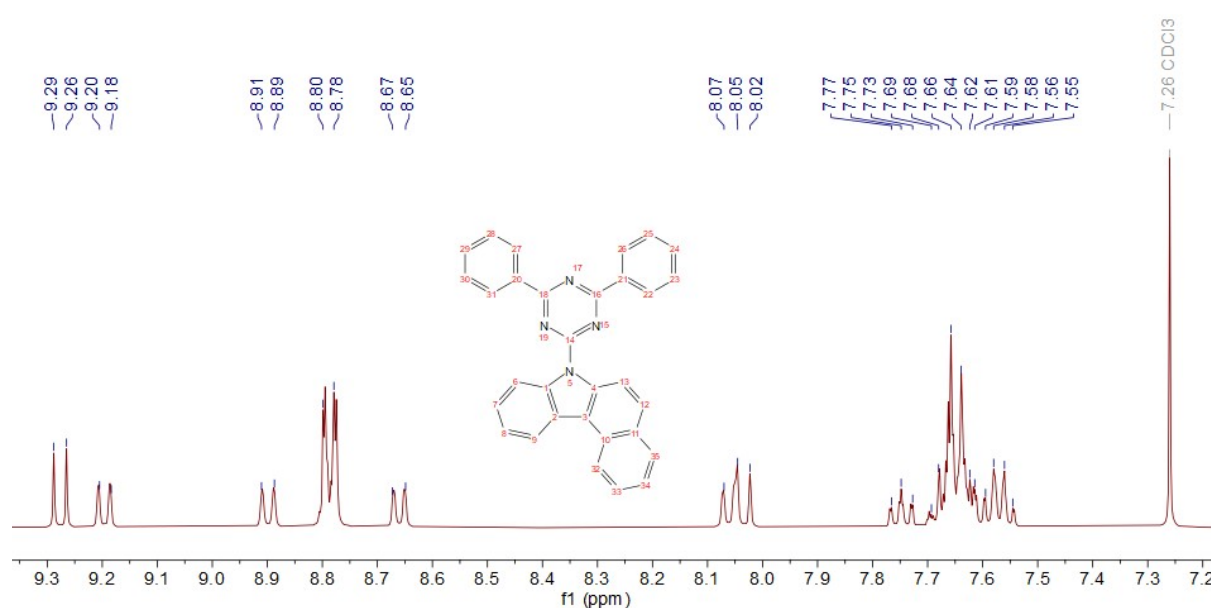


Figure S1. ¹H-NMR spectrum of DPhBCzT in CDCl₃.

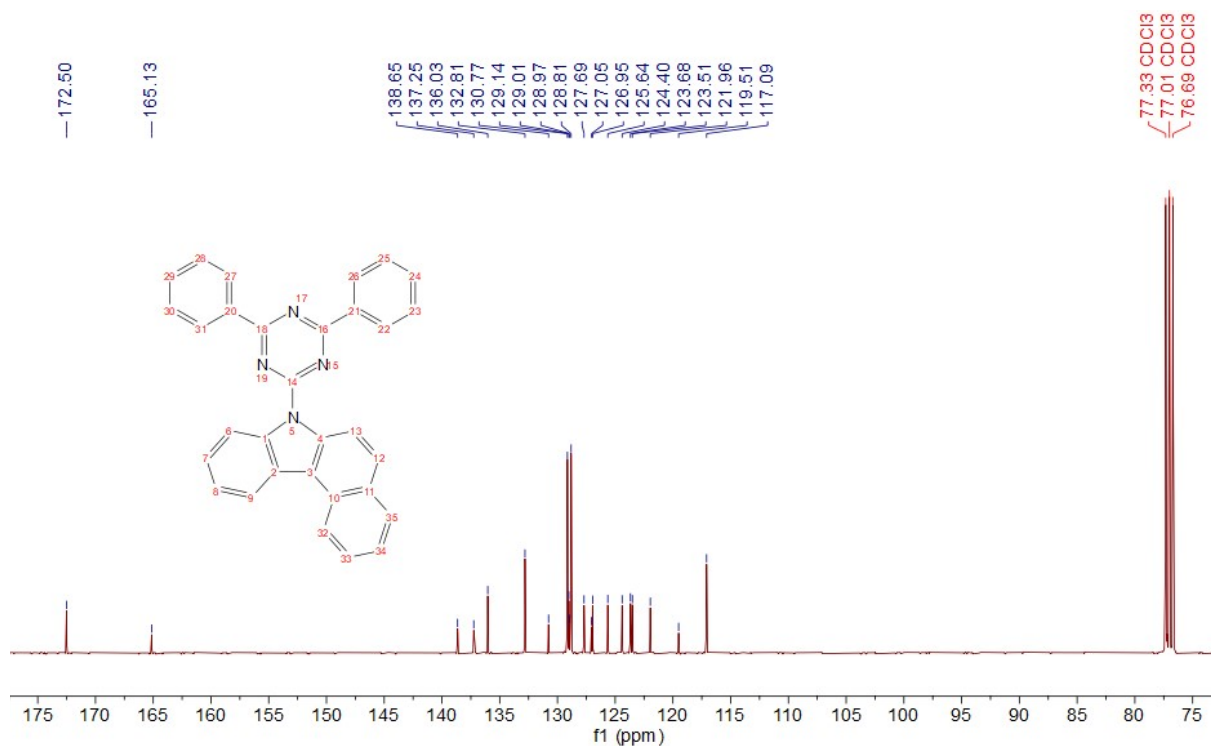


Figure S2. ¹³C-NMR spectrum of DPhBCzT in CDCl₃.

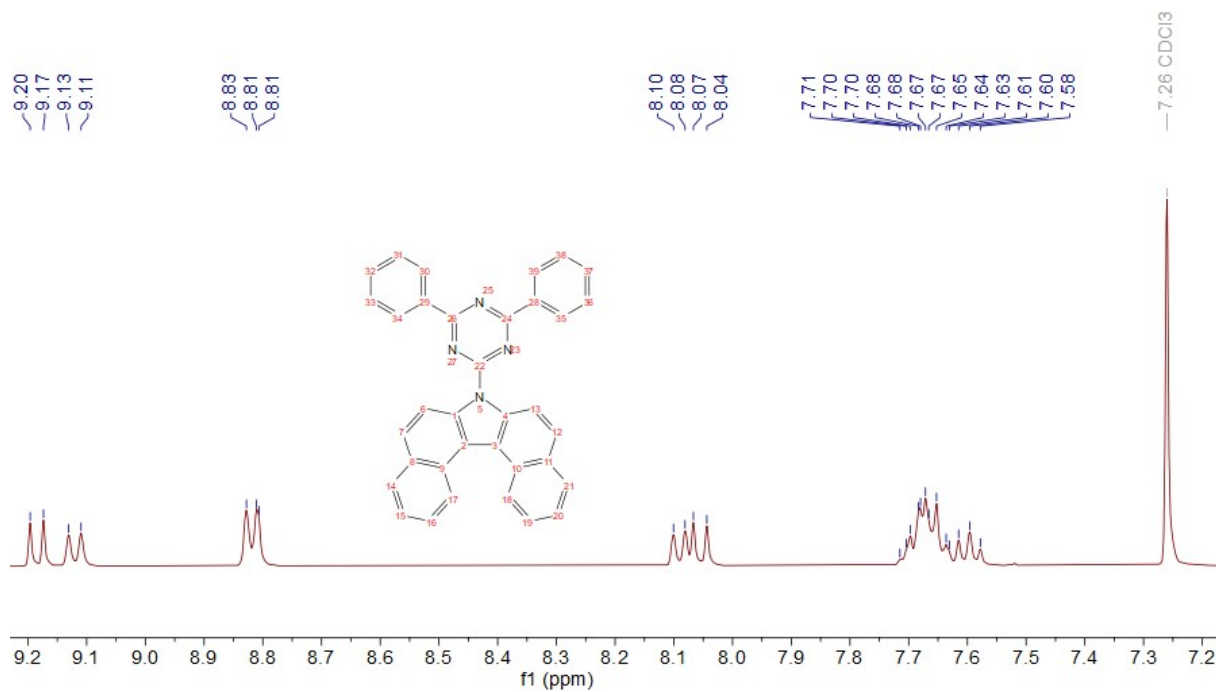


Figure S3. ¹H-NMR spectrum of DPh₂BCzT in CDCl₃.

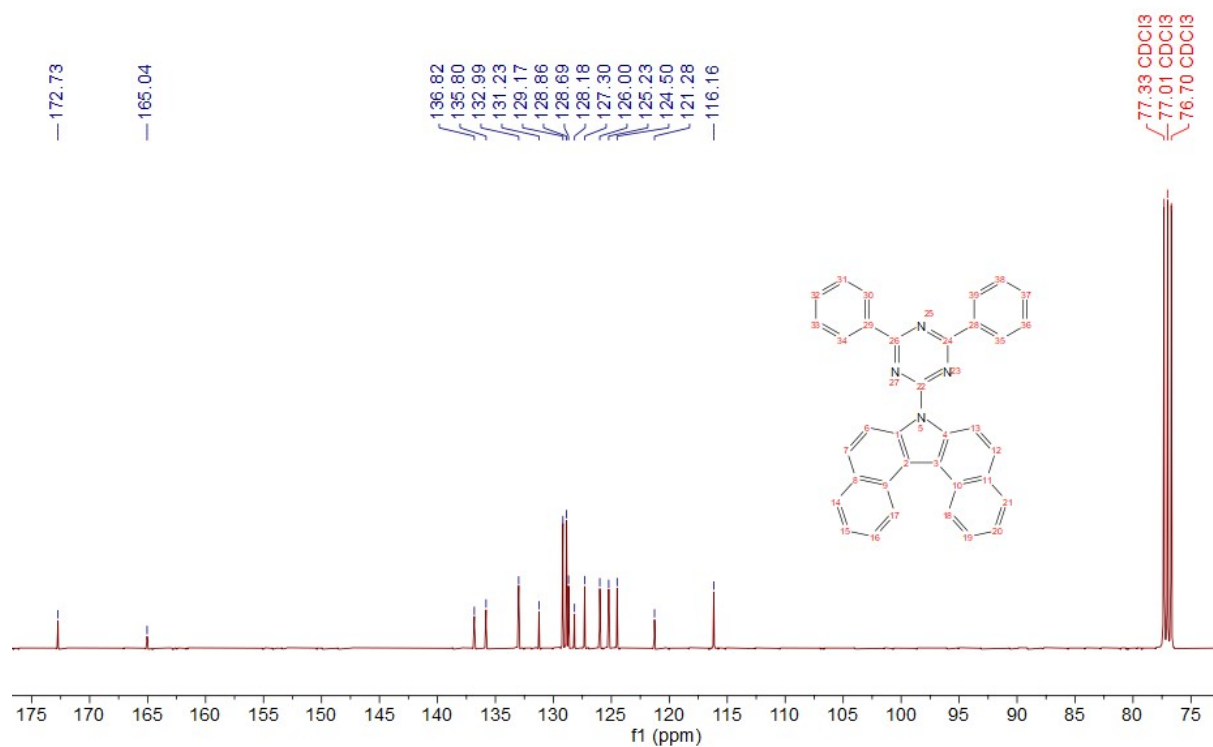


Figure S4. ¹³C-NMR spectrum of DPh₂BCzT in CDCl₃.

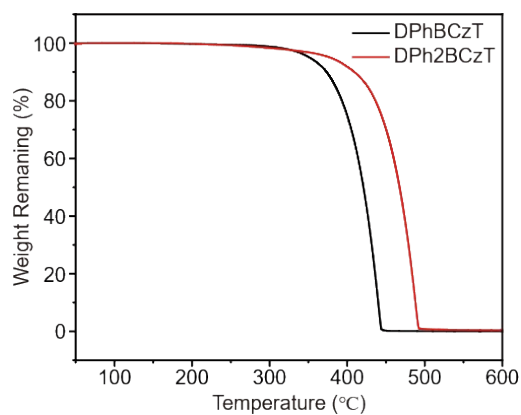


Figure S5. TGA curves of DPhBCzT and DPh₂BCzT.

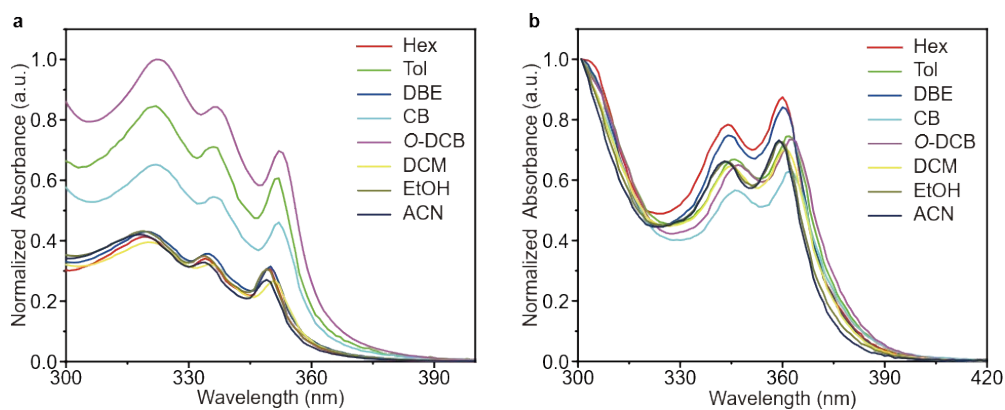


Figure S6. Normalized UV absorption spectra of a) DPhBCzT and b) DPh₂BCzT in different solvents (1×10^{-5} M).

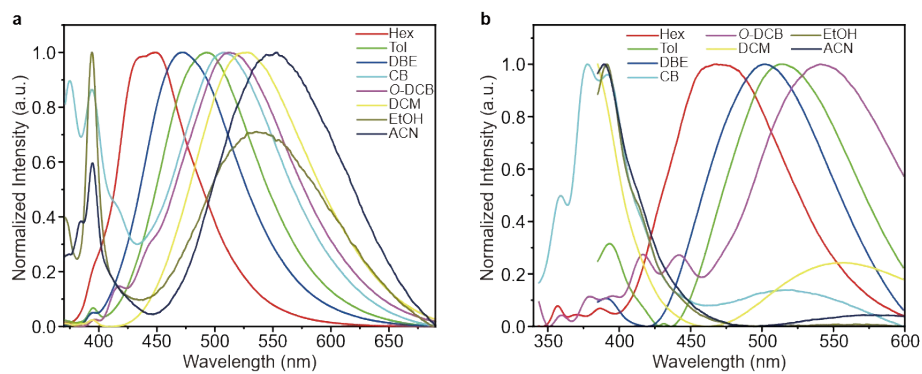


Figure S7. Normalized SSPL spectra of a) DPhBCzT and b) DPh2BCzT in different solvents (1×10^{-5} M).

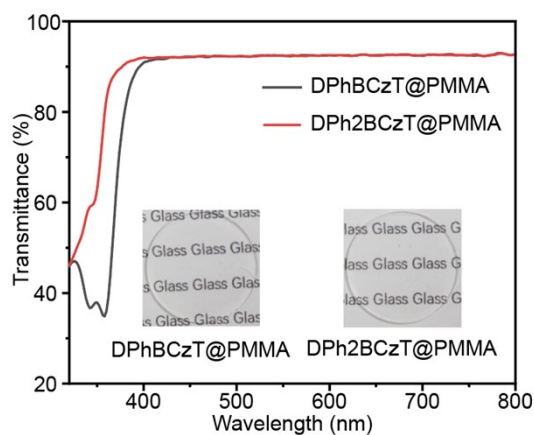


Figure S8. Transmittance spectra and photographs (insets) of DPhBCzT@PMMA and DPh2BCzT@PMMA films.

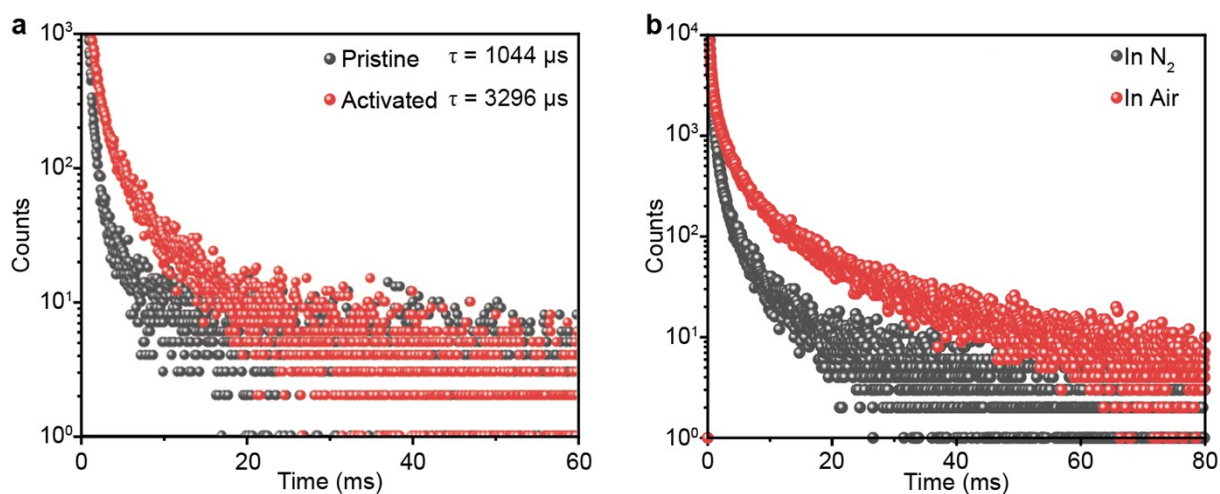


Figure S9. a) Decay profiles of the 450 nm emission of DPhCzT@PMMA film in air before (pristine) and after (activated) photoactivation; b) Decay profiles of the 450 nm emission of photoactivated DPhCzT@PMMA film in different atmospheres at room temperature.

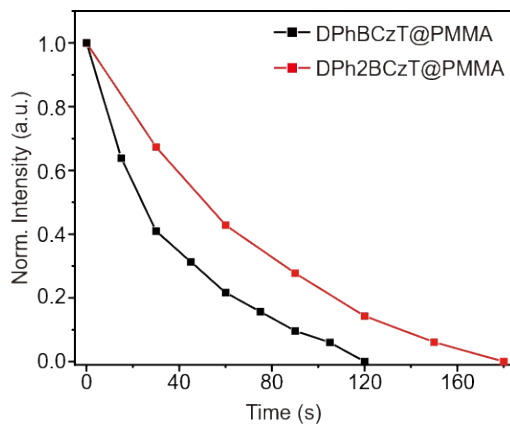


Figure S10. Deactivation of the RTP emission of DPhBCzT@PMMA and DPh2BCzT@PMMA films at 500 and 560 nm respectively in air at room temperature.

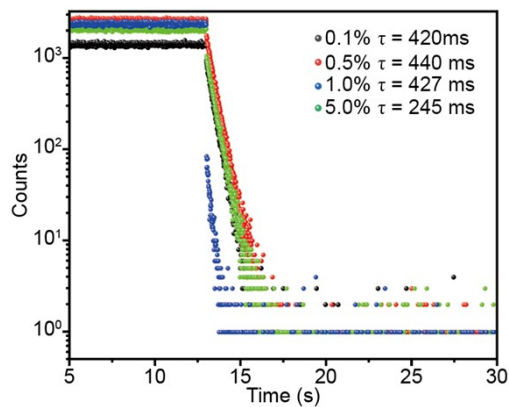


Figure S11. Decay profiles of the 560 nm emission of photoactivated DPh2BCzT@PMMA film with different weight doping contents measured by kinetic scanning.

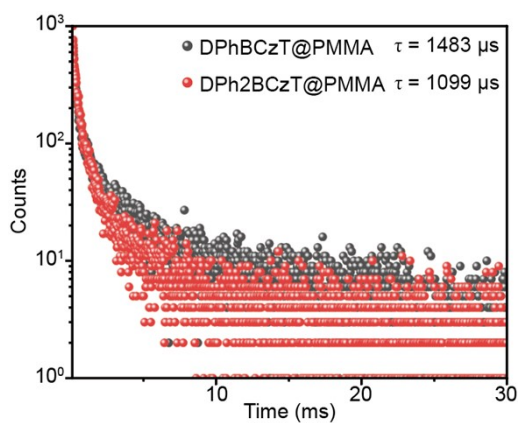


Figure S12. Decay profiles of the emissions of pristine DPhBCzT@PMMA and DPh2BCzT@PMMA films at 510 and 560 nm respectively.

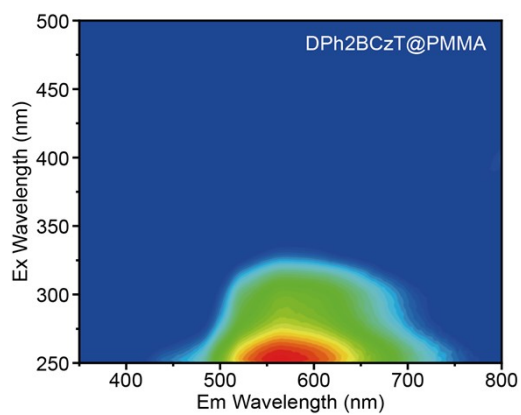


Figure S13. 2D excitation-SSPL mapping of the pristine DPh2BCzT@PMMA film.

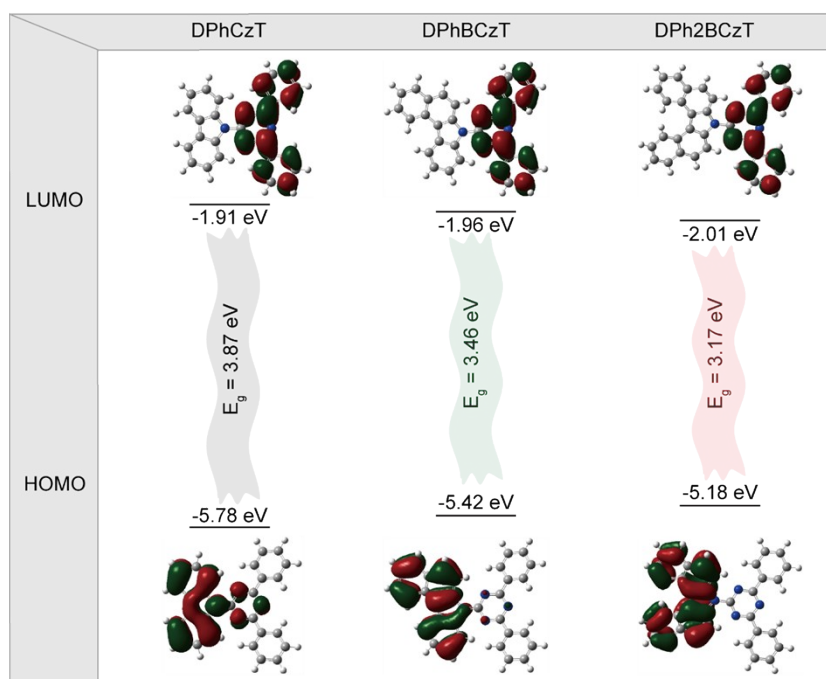


Figure S14: DFT predicted frontier molecular orbital energy levels and distributions of DPhCzT, DPhBCzT and DPh2BCzT.

8. Tables

Table S1. The single crystal data of DPhBCzT.

Compound	DPhBCzT
Empirical formula	C ₃₁ H ₂₀ N ₄
Formula weight	448.51
Temperature	293 K
Crystal system	monoclinic
Space group	I2/a
Unit cell dimensions	a = 20.6286(8) Å; alpha = 90 deg. b = 5.2262(16) Å; beta = 102(4) deg. c = 41.3488(16) Å; gamma = 90 deg.
Volume	4356.5(3)
Z	8
Density (calculated)	1.368 g/cm ³
Absorption coefficient	0.641 mm ⁻¹
F (000)	1872.0
CCDC number	2488067

Table S2. Photophysical properties of the photoactivated DPhBCzT@PMMA and DPh2BCzT@PMMA films with different doping contents.

Dopant	Doping content (wt%)	PLQY (%)	RTP lifetime (ms)
DPhBCzT	0.1	0.47	883
DPhBCzT	0.5	3.40	1000
DPhBCzT	1.0	2.48	1021
DPhBCzT	5.0	2.44	<1
DPh2BCzT	0.1	3.17	420
DPh2BCzT	0.5	2.31	440
DPh2BCzT	1.0	3.99	427
DPh2BCzT	5.0	0.57	245

Reference

1. Qian, C. *et al.* Carbazole&benzoindole-based purely organic phosphors: A comprehensive phosphorescence mechanism, tunable lifetime and an advanced encryption system. *J. Mater. Chem. C* **9**, 14294–14302 (2021).

2. Li, C. *et al.* Achieving efficient organic room-temperature phosphorescence through acceptor dendronization. *J. Am. Chem. Soc.* **147**, 18317–18326 (2025).
3. An, Z. *et al.* Conjugated asymmetric donor-substituted 1,3,5-triazines: New host materials for blue phosphorescent organic light-emitting diodes. *Chem. – Eur. J.* **17**, 10871–10878 (2011).
4. An, Z. *et al.* Stabilizing triplet excited states for ultralong organic phosphorescence. *Nat. Mater.* **14**, 685–690 (2015).
5. Zhang, Y. *et al.* Enhanced photoactivated circularly polarized afterglow with high dissymmetry factor and tunable emission. *Adv. Funct. Mater.* **35**, 2424404 (2025).
6. Zeng, M. *et al.* Enabling robust blue circularly polarized organic afterglow through self-confining isolated chiral chromophore. *Nat. Commun.* **15**, 3053 (2024).